Bioconjugate Chemistry

Article

pubs.acs.org/bc

Supramolecular Surface Immobilization of Knottin Derivatives for Dynamic Display of High Affinity Binders

Shrikrishnan Sankaran,[†,§,⊥] Mark de Ruiter,[‡,⊥] Jeroen J. L. M. Cornelissen,[‡] and Pascal Jonkheijm*[,†,§]

[†]Molecular Nanofabrication Group and [‡]Biomolecular Nanotechnology Group of the MESA+ Institute for Nanotechnology, University of Twente, P.O. Box 217, 7500 AE Enschede, The Netherlands

[§]Bioinspired Molecular Engineering Laboratory of the MIRA Institute for Biomedical Technology and Technical Medicine, University of Twente, 7500 AE Enschede, The Netherlands

Supporting Information

ABSTRACT: Knottins are known as a robust and versatile class of miniprotein scaffolds for the presentation of high-affinity binding peptides; however, to date their application in biomaterials, biological coatings, and surface applications have not been explored. We have developed a strategy to recombinantly synthesize a β-trypsin inhibitory knottin with supramolecular guest tags that enable it to adhere to self-assembled monolayers of the supramolecular host cucurbit[8]uril (CB[8]). We have described a strategy to easily express knottins in *E. coli* by conjugating them to a fluorescent protein after which they are cleaved and purified. Knottin constructs that varied in the number and position of the supramolecular tag at either the N- or C-termini or at both ends have been verified for their trypsin inhibitory function and CB[8]-binding properties in solution and on surfaces. All of the knottin constructs showed strong inhibition of trypsin with inhibition constants between 10 and 30 nM. Using microscale thermophoresis, we determined that the supramolecular guest tags on the knottins bind CB[8] with a K_d of ~6 μM in solution. At the surface, strong divalent binding has been determined with a K_d of 0.75 μM in the case of the knottin with two supramolecular guest tags, whereas only weak monovalent binding occurred when only one guest tag was present. We also show successful supramolecular surface immobilization of the knottin using CB[8] and prove that they can be used to immobilize β-trypsin at the surface.

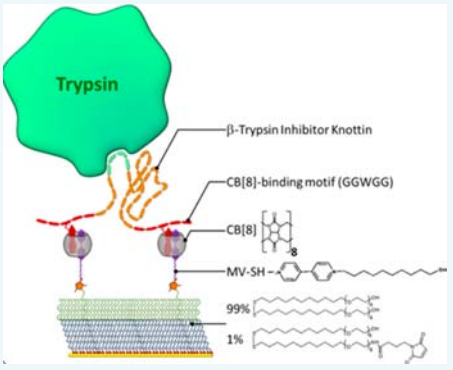

INTRODUCTION

Knottins are a very interesting class of miniproteins since their cystine-stabilized knot structure not only confers upon them very high thermal stability and resistance against proteolytic enzymes but also allows for extensive modification of the peptide sequences on their loops.[1] Apart from the disulfide-bridge forming cysteines and a few other stabilizing amino acids, the residues on the loops can almost be completely changed.[2] Taking advantage of these properties, nature has produced hundreds of knottins with very high activities as protease inhibitors, neurotoxins in spider and scorpion venom, insecticides from plants, and antimicrobial agents as can be seen in the open access online knottin database.[3,4] Several of these naturally occurring knottins have also been tested as possible analgesics, antimalarials, and pesticides.[5]

The potential of these simple proteins to be stable molecular scaffolds has promoted their extensive usage in phage and bacterial display systems to identify high affinity binding peptides for various target proteins related to growth factors, cancer, HIV, and *in vivo* imaging.[6] These display techniques, combined with the fact that their small size enables them to be chemically synthesized, have hailed these molecules as potential substitutes for antibodies.[7,8] Daugherty and co-workers have successfully developed a simple bacterial display system by which they were able to determine high affinity binding knottins toward thrombin and neuropilin.[9,10] Chiche et al. have developed a truncated form of the knottin EETI-II, called Min-23, with which they were able to identify high affinity binders for various target proteins.[11,12] Similarly, phage display systems have been used to identify modified Min-23 miniproteins that were able to bind growth factors such as vascular endothelial growth factor (VEGF).[13,14] Cochran and co-workers, through rational design strategies, developed knottins containing peptide sequence Arg-Gly-Asp (RGD) with flanking residues that were able to bind different integrins with different levels of affinity.[15,16] Further, to expand upon the functionality of the exposed groups, strategies have been developed to chemically conjugate various synthetic molecules and non-natural amino acids.[17,18] Such constructs have been successfully shown as effective imaging agents using conjugated fluorescent dyes and radiofluorinated compounds.[19,20]

Because of such possibilities of effectively displaying a wide variety of peptide sequences made of either natural or non-natural amino acids, these miniprotein scaffolds are excellent

Received: July 27, 2015
Revised: August 12, 2015
Published: August 13, 2015

DOI: 10.1021/acs.bioconjchem.5b00419
Bioconjugate Chem. 2015, 26, 1972−1980

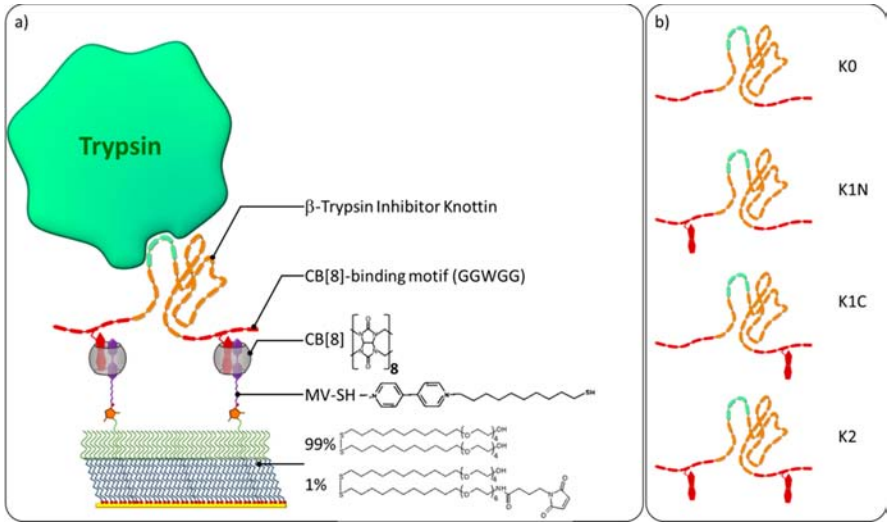

Figure 1. (a) Schematic depicting the supramolecular surface immobilization of a genetically modified functional β-trypsin inhibitor knottin onto a CB[8]-presenting SAM on gold. (b) Depictions of the four different CB[8]-binding knottin constructs used in this study. The presence of tryptophan (W) in the CB[8]-binding motif (red) is represented by its indole side chain.

candidates for fabricating highly stable bioactive surfaces and materials for research, biosensors and even implants. Their loop structure would also ensure better solvent exposure of the incorporated peptide sequences, and their size (3−5 kDa) allows for tighter oriented packing than antibodies and nanobodies.[21] Since they contain only about 30 amino acids that fold into a tight cage-like structure, nonspecific interactions with surfaces and proteins are also substantially reduced compared to larger constructs. However, so far, there are no studies attempting to fabricate biofunctional surfaces using knottins.

Several strategies have been explored to incorporate various other functional molecules at surfaces, for example, using self-assembled monolayers (SAMs), polymers, nanoparticles, lipid bilayers, etc.[22,23] Furthermore, supramolecular chemistry has enabled the introduction of dynamics and responsiveness in these functional surfaces.[24,25] These platforms are also developing as powerful tools for studying complex biological processes such as cellular adhesion, migration, cell−cell interactions, etc.[26] In particular, synthetic host−guest systems have recently been vigorously explored for these purposes due to their similarity to protein−protein interactions found in nature.[27] By careful design of the host−guest components, spatial and temporal control of the interactions can be introduced.[28,29] Stupp and co-workers have been able to create a matrix, using alginate and β-cyclodextrin, with controllable cell-adhesion properties by competitive exchange of functionalized guest molecules.[30] We had previously developed a supramolecular platform for the photoresponsive display of bioactive ligands using azobenzene glycoconjugates and β-cyclodextrin SAMs.[31] We were also able to develop a supramolecularly addressable bacterial strain and incorporate it as a living component with SAMs bearing cucurbit[8]uril (CB[8]) host molecules.[32] In order to accomplish this, we genetically modified one loop of a Min-23 miniprotein to carry a CB[8]-binding motif. This was then linked to a transmembrane protein so that it would get displayed on the bacterial surface. The bacterial display system clearly showed specific binding toward CB[8], causing aggregation of bacteria in solution through multivalent interactions and allowing the adhesion of bacterial cells onto CB[8] SAMs while still retaining their motility. This study highlighted the potential of developing knottins with supramolecular functionalities.

In the past decade, there has been a keen interest in exploring the possibility of applying the CB[n] family of host molecules for biomedical applications. CB[n]s are hollow pumpkin shaped macrocyclic molecules made of glycouril monomer units.[33] They have a hydrophobic cavity and polar rims lined with ureido-carbonyl oxygens allowing them to bind a variety of aromatic cations with micromolar affinities.[34,35] Among the CB[n] family members, CB[8] happens to be especially interesting since the cavity is large enough to simultaneously encapsulate two aromatic guest molecules.[36] This enables the possibility to construct, e.g., dual responsive nanoparticle systems when two different guest molecules that are affected by different external stimuli are included in the cavity.[37] We and others have developed strategies to assemble CB[8] on biologically relevant surfaces.[29,38,39] Furthermore, we have also demonstrated the ability to dynamically display bioactive ligands for cell adhesion and triggered release using electrochemical stimuli.[29,40] These studies indicate the potential of CB[8] for developing highly dynamic and responsive smart surfaces for biomedical applications and research.

Here, we have explored the possibility of constructing knottins that can be specifically immobilized on CB[8] monolayers and still bind their target protein (Figure 1a). A strategy was developed to recombinantly synthesize a β-trypsin inhibitor knottin with supramolecular guest tags that enable it to adhere to SAMs of CB[8]. The peptide sequence "GGWGG" has been shown to bind CB[8] with low micromolar affinities,[41] and we designed four different knottin constructs (K) bearing this motif at either the N-terminus (K1N), C-terminus (K1C), both termini (K2), or none (K0) (Figure 1b). In the cases of K1N, K1C, and K0, the termini without the GGWGG motif have GGGGG motifs instead. First, we describe a strategy to easily express these knottins in *E. coli* by conjugating them to a fluorescent protein after which it is cleaved and purified. These knottins were proven to be functional using a trypsin inhibitor assay, and their CB[8]-binding characteristics in solution were compared. We also tested supramolecular surface immobilization of these knottin using CB[8] and prove that even at the surface, these

DOI: 10.1021/acs.bioconjchem.5b00419
Bioconjugate Chem. 2015, 26, 1972−1980

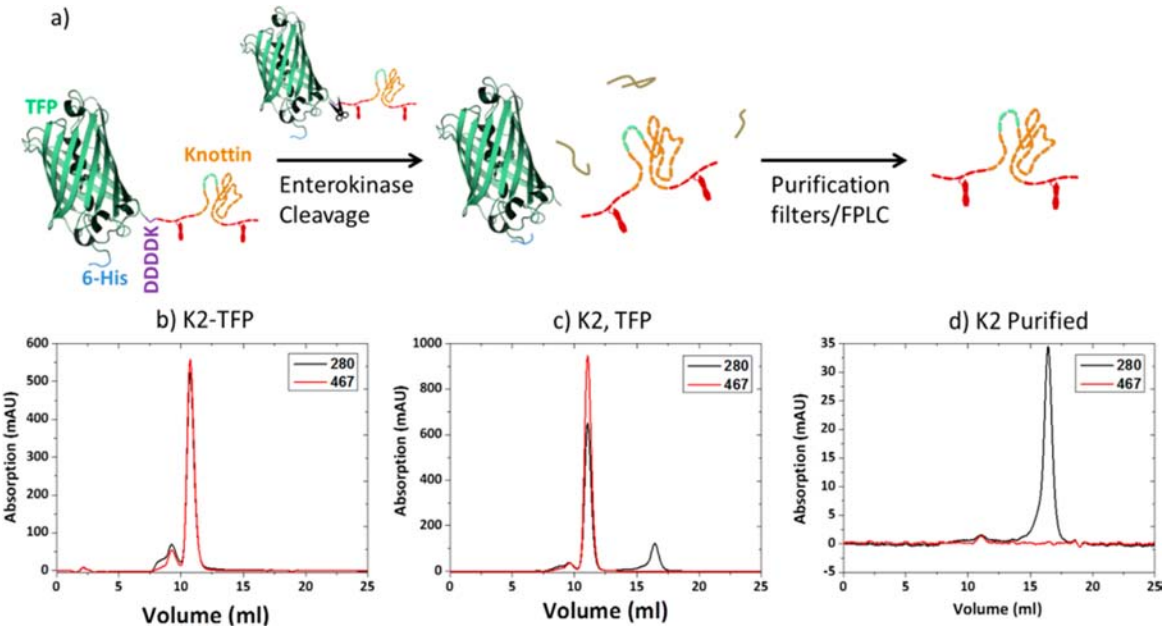

Figure 2. (a) Schematic representation of the steps involved in synthesizing and purifying the knottin constructs. Size exclusion FPLC traces of (b) the recombinantly synthesized fusion protein (K2-TFP), (c) the protein mixture (K2 and TFP) after enterokinase cleavage, and (d) K2 knottin purified using centrifugal filter units.

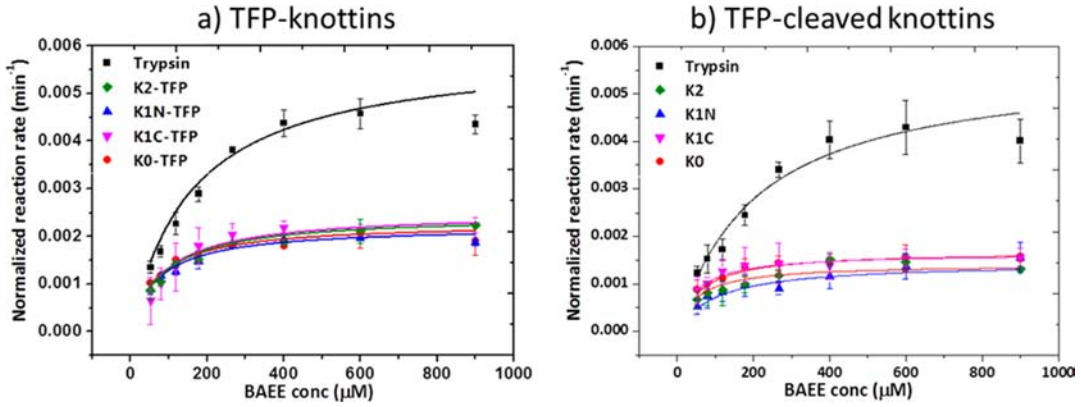

Figure 3. Trypsin inhibition assay following the cleavage of different concentrations of BAEE by β-trypsin in the absence and presence of the different knottin constructs in (a) TFP-fused and (b) TFP-cleaved knottins. Data are presented as the mean ± STD, n = 3. Solid lines represent fitting of the individual curves using Michaelis–Menten eq 1. K_{iapp} values obtained using eq 2 of K2-TFP = 29 ± 5 nM, K1N-TFP = 22 ± 3 nM, K1C-TFP = 31 ± 8 nM, K0-TFP = 24 ± 6 nM, K2 = 8 ± 4 nM, K1N = 9 ± 2 nM, K1C = 12 ± 5 nM, and K0 = 12 ± 4 nM.

miniproteins show functionality. For the first time, the binding of a functional bivalent guest molecule (K2) has been studied in comparison to monovalent guests (K1C/N) on such ternary complex based SAMs. The bivalent guest had a higher binding affinity and was the only one with which trypsin was clearly immobilized on the supramolecular surface.

RESULTS AND DISCUSSION

Design and Recombinant Synthesis of Knottins. As shown in Figure 2a, we developed a modified strategy to express and purify our knottin constructs. Because of their multiple cysteines and poor solubility during expression in *E. coli*, knottins are usually formed in inclusion bodies from which they must be solubilized, denatured, and refolded. Kolmar and co-workers developed a strategy to circumvent this problem by fusing the knottin to barnase, which improved solubility and caused it to be secreted into the periplasm where disulfides form more easily in an oxidative environment.[42] On the basis of these concepts, we devised a modified strategy to further improve the solubility and folding of our knottin constructs. Solubility was improved by genetically fusing the knottins to the C-terminal of a His_6-tagged teal fluorescent protein (TFP) with a linker containing an enterokinase cleavage site (DDDDK). Furthermore, TFP was chosen since it allowed us to visualize the protein and perform fluorescence based analysis. Disulfide bond formation was improved (as shown by Ellman's reagent) by expressing these constructs in Rosetta Gami 2 *E. coli* cells, a specially engineered commercially available strain in which certain thioreductases are mutated. These fusion proteins were purified using Ni-NTA affinity columns and characterized using SDS–PAGE (Figure S1, Supporting Information) and size-exclusion FPLC (Figure 2b (K2) and Figure S2a (K0, K1N, K1C, and K2)). We were able to obtain an average of 34 mg of these fusion proteins (~4.7 mg knottin) from 1 L of bacterial culture. Next, enterokinase was used to cleave the knottin from the TFP (Figure 2c). As expected, the absorbance

DOI: 10.1021/acs.bioconjchem.5b00419
Bioconjugate Chem. 2015, 26, 1972–1980

at λ = 280 nm varied for each construct, depending on the number of tryptophan residues present, K2 showing the highest and K0 showing the least (Figure S2a). Surprisingly, each knottin construct eluted at different volumes during size exclusion chromatography even though their sizes are not considerably different (Figure S2a). K2 eluted at 16 mL, K1N and K1C at 15 mL, and K0 at 14 mL indicating that the secondary structure of K2 was the smallest followed by K1N and K1C and that K0 was the bulkiest. This was a counterintuitive outcome since the molecular weights of these constructs, verified by MALDI-TOF analysis (Figure S2b), followed the trend of K2 > K1N = K1C > K0 due to the presence of the tryptophan residues. The most likely explanation for this behavior is that the indole side chains of tryptophan, being hydrophobic, fold into the hydrophobic core of the knottin causing these constructs to be more compact. Because of the considerable difference in size between the knottins (~4.8 kDa) and the His_6-tagged TFP (~27 kDa) (Figure 2c), they were separated using a centrifugal filter unit with a 10 kDa cutoff. Smaller impurities were removed using a centrifugal filter unit with a 3 kDa cutoff. Knottins purified in this manner were analyzed by FPLC (Figure 2d) and MALDI-TOF (Figure S2b) and indicated a lack of free thiols (Ellman's reagent). The enterokinase cleavage and purification steps resulted in nearly a 70% yield of pure knottin providing us with an average of 3.2 mg of purified knottins per 1 L of bacterial culture, which is comparable to yields reported by Kolmar and co-workers,[42] yet production and cleavage were easier in the presence of TFP while the TFP-fused knottins can be used for subsequent detailed fluorescent based binding studies.

Evaluating Trypsin Inhibitory Functionality of Knottin Constructs. To ensure that our purified knottin constructs were still functional, we performed a trypsin inhibitor assay (Figure 3). For this purpose, we followed the cleavage of Nα-benzoyl-L-arginine ethyl ester (BAEE) by measuring the emerging absorbance at λ = 260 nm over time. It was clearly seen that the rate of cleavage reduced in the presence of the knottins. Since our knottins are known to inhibit β-trypsin by blocking its active site,[43] competitive inhibition kinetics would be expected where inhibited reactions have the same V_{max} value as the uninhibited reactions but a lower K_m value. However, fitting all plots with the Michaelis–Menten eq 1 revealed that the presence of knottins caused a considerable drop in both the V_{max} and K_m values (Table S1).

$$v = \frac{V_{max}[S]}{K_m[S]} \tag{1}$$

where v is the reaction rate (s^{-1}), V_{max} is the maximum reaction rate (s^{-1}), $[S]$ is the BAEE concentration (M), and K_m is the Michaelis constant (M), i.e., the concentration of BAEE where the reaction rate is half of V_{max}.

This effect could correspond to noncompetitive inhibition or irreversible inhibition. Noncompetitive inhibition is highly unlikely since the knottins are known to bind and block the active site of β-trypsin. Also, since the inhibition occurs at much lower inhibitor concentrations than that of BAEE, high binding strength is expected, suggesting irreversible inhibition. However, in the case of irreversible inhibition kinetics, it is known that V_{max} of the inhibited reaction drops compared to that of the uninhibited reaction but that K_m stays the same. This indicated that the high binding affinity of these knottins must have resulted in pseudoirreversible inhibition kinetics. Consequently, apparent inhibitor constants were determined with the following formula eq 2, which describes the case of competitive tight binding inhibitors:[42,44]

$$\frac{V_i}{V_o} = \frac{[E_T] + [I_T] + K_{iapp} - \{([E_T] + [I_T] + K_{iapp})^2 - 4[E_T][I_T]\}^{1/2}}{2[E_T]} \tag{2}$$

where V_i and V_0 are the V_{max} values of the inhibited and uninhibited reactions, respectively, $[E_T]$ is the total concentration of β-trypsin, $[I_T]$ is the total knottin concentration, and K_{iapp} is the apparent dissociation constant of the enzyme–inhibitor complex. This analysis provided K_{iapp} values in the low nanomolar range, similar to values obtained by Kolmar and co-workers for recombinantly produced β-trypsin-inhibitor knottins.[42] Interestingly, the cleaved knottins showed a modest improvement in K_{iapp} values (~10 nM) compared to that of the TFP-fused knottins (~26 nM) presumably due to reasons of steric hindrance. These results indicated that all four knottin constructs exhibited significant trypsin inhibitory functionality.

Evaluating CB[8] Binding Capability of Knottin Constructs. The CB[8] binding capability of the different knottin constructs in solution was tested using microscale thermophoresis (MST). In this technique, a solution containing a fluorescent species is locally heated, and the diffusion rate of the molecules in that spot is determined by measuring the fluorescence intensity. The diffusion rate depends on the hydration shell around the fluorescent molecule, and when a binding event occurs, this shell gets modified, resulting in a different rate of diffusion. For this purpose, we used the TFP-fused knottin constructs and measured the binding affinity by titrating with a range of CB[8] concentrations (2 nM–37.5 μM) in the presence of 150 μM methylviologen (MV^{2+}) (Figure 4a). MV^{2+} forms a 1:1 binary complex with CB[8] allowing us to study the affinity of the knottins with this complex to form a ternary complex. Under these conditions, K1N-TFP, K1C-TFP, and K2-TFP clearly exhibited changes in thermophoretic behavior with increasing CB[8] concentrations. K0-TFP did not show such changes in diffusion rate indicating that the CB[8]-MV^{2+} complex binds specifically to the

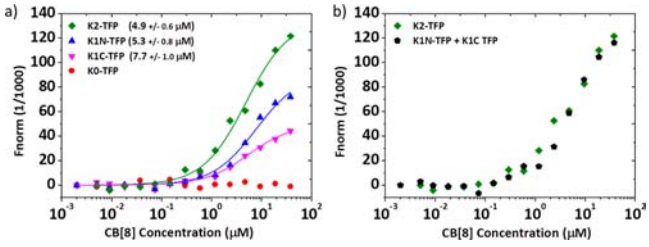

Figure 4. (a) Thermophoretic binding curves corresponding to the interaction between the different TFP-Fused knottins and the CB[8]-MV^{2+} complex. Solid lines represent fitting of the data with a Langmuir equation, and the values in parentheses in the legend are the obtained dissociation constants. (b) Thermophoretic binding curves of K2-TFP and the sum of K1N-TFP and K1C-TFP.

DOI: 10.1021/acs.bioconjchem.5b00419
Bioconjugate Chem. 2015, 26, 1972–1980

GGWGG motif on the other constructs at these concentrations. The low micromolar binding affinities (~6 μM) determined are in the expected range for such supramolecular host–guest interactions.[41] No significant differences were observed between the binding affinities of the monovalent binding constructs (K1N-TFP and K1C-TFP) and the bivalent construct (K2-TFP) since the CB[8]-MV^{2+} complex still interacts with the GGWGG motifs in a monovalent manner. However, the thermophoretic amplitudes of K2-TFP were almost equal to the sum of the values of K1N-TFP and K1C-TFP at each point (Figure 4b). This indicates the possibility of the simultaneous binding CB[8]-MV^{2+} complexes with both the GGWGG motifs on K2-TFP. Differences in thermophoretic amplitudes between K1N-TFP and K1C-TFP arise due to the fact that the CB[8]-MV^{2+} complex binds these proteins at different locations.

Supramolecular Surface Immobilization of Knottins. Confident that the knottin constructs showed an inhibitory effect on trypsin and were able to bind CB[8], we proceeded to study the valency of their interaction with CB[8] SAMs using surface plasmon resonance (SPR). For this purpose, we used monolayers that display MV^{2+} on a background of nonfouling tetraethylene glycols, as depicted in Figure 1a.[40] CB[8] was first noncovalently immobilized onto the MV^{2+} units, and then the knottins were allowed to interact with this complex. From Figure 5a, it can be seen that the knottins with only one

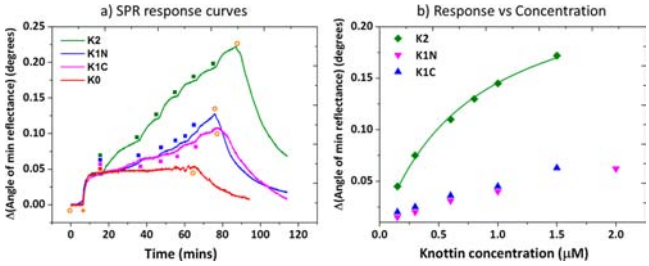

Figure 5. (a) SPR response curves corresponding to the binding of each knottin construct on CB[8] SAMs. Open circles (○) represent the buffer, filled circles (orange circle) represent 50 μM CB[8], solid squares (green, blue, purple, and red) represent increasing concentrations of the corresponding knottin constructs (K0, 1 μM; K1N; 0.15, 0.3, 0.6, 1, 2, and 3 μM; K1C, 0.15, 0.3, 0.6, 1, and 1.5 μM; and K2, 0.15, 0.3, 0.6, 0.8, 1, and 1.5 μM). Titration of various knottin constructs were always performed in the presence of 50 μM CB[8] in solution. (b) Saturating SPR response for each concentration of K2 and the corresponding maximum SPR response of K1N and K1C for the same time interval at each concentration. The solid line represents the fitting of K2 values to the Langmuir adsorption equation (K_d = 0.75 ± 0.06 μM).

GGWGG motif (K1N and K1C) show weaker binding compared to that of K2 at the concentrations used (0.15–3 μM). At higher concentrations up to 30 μM, even with Tween-20 added, the knottin solutions become turbid over time signified by broadening in the UV/vis absorption spectrum (Figure S3). This indicated aggregation of knottins into clusters possibly due to their relatively poor water solubility. Tween-20 was added as a nonionic amphiphilic detergent used for solubilizing membrane proteins. It can prevent protein clustering by masking hydrophobic domains. It has also been extensively used to prevent nonspecific binding in protein–protein interactions, for example, in immunoassays. However, irrespective of the position of the supramolecular guest tag, either at the N- or C-terminus, the SPR binding profile was nearly identical. K0 did not exhibit surface adhesion confirming that immobilization of the other constructs occurred only through specific interactions between CB[8] and the GGWGG motif in agreement with the MST results in solution. When maximum SPR responses of K2 were plotted against corresponding concentrations and fitted with the Langmuir adsorption equation, assuming both GGWGG motifs can simultaneously bind to the CB[8] SAM, a dissociation constant (K_d) of 0.75 ± 0.06 μM was obtained (Figure 5b). This value is lower than the binding constant of a single GGWGG motif to the CB8-MV^{2+} complex. This improvement in binding affinity due to divalent interactions is comparable to what has been reported with similar supramolecular host–guest systems in buffered conditions with Tween-20.[45] Binding plots of K1N and K1C indicated that their binding was still in the linear regime at these concentrations (0.15–3 μM), confirming less stable binding between the monovalent constructs and CB[8] SAMs. This difference in binding strength was also observed when rinsing the surfaces with buffer. The divalent K2 construct was only partly removed, while the monovalent constructs (K1N and K1C) were completely removed in the same period of time. The signal of the divalent K2-TFP drops to nearly half of its saturation value in ca. 14 min. Surface adhesion of TFP-fused knottin constructs were also followed using SPR (Figure S4). Even though significant nonspecific adhesion was seen with K0-TFP, which could not be prevented by adding Tween-20, better surface adhesion was clearly seen with the bivalent K2-TFP compared to that of the monovalent K1N-TFP and K1C-TFP. Nonspecific adhesion most likely occurs due to multiple weak interactions between CB[8] and the solvent-exposed aromatic amino acids present in the fluorescent proteins as observed before by others.[46] These results collectively indicate that specific supramolecular host–guest binding occurs between the surface and the knottin constructs after cleaving off the TFP parts and confirm that a divalent interaction occurs in the assembly of the K2 knottin constructs onto CB[8] SAMs.

To test the applicability of the CB[8]-binding knottins in fabricating dynamic protein arrays, we attempted patterning them by supramolecular microcontact printing.[47] First, we tested whether the knottin constructs would bind specifically to noncovalent arrays of CB[8]. For this purpose, circle-patterns of CB[8] were first printed on surfaces displaying MV^{2+}. To visualize knottin adhesion, we incubated these surfaces with the TFP-fused knottins. Fluorescent arrays were clearly seen in the cases of K1N-TFP, K1C-TFP, and K2-TFP but not with K0-TFP as shown in Figure 6a. As a second check to verify specific surface adhesion following ternary complex formation, we used CB[7] as a negative control. Since CB[7] has a smaller cavity, it can accommodate only one guest at a time.[34] Consequently, CB[7] should be able to bind to MV^{2+} at the surface but not form a ternary complex with the knottins. As expected, we did not observe any fluorescent arrays after incubating all four TFP-fused knottins with CB[7]-patterned surfaces.

As the knottin constructs adhere to CB[8]-arrays, dissociation of CB[8] is expected to occur in parallel, resulting in the weakly fluorescent arrays seen in Figure 6a. To increase the density of the bound knottins and simplify the process of making such arrays, we tested a different strategy. Mixtures of CB[8] and the TFP-fused knottins were printed on surfaces displaying MV^{2+} followed by a 20 min wash in buffer with mild shaking. In Figure 6b, it can be seen that after printing,

DOI: 10.1021/acs.bioconjchem.5b00419
Bioconjugate Chem. 2015, 26, 1972–1980

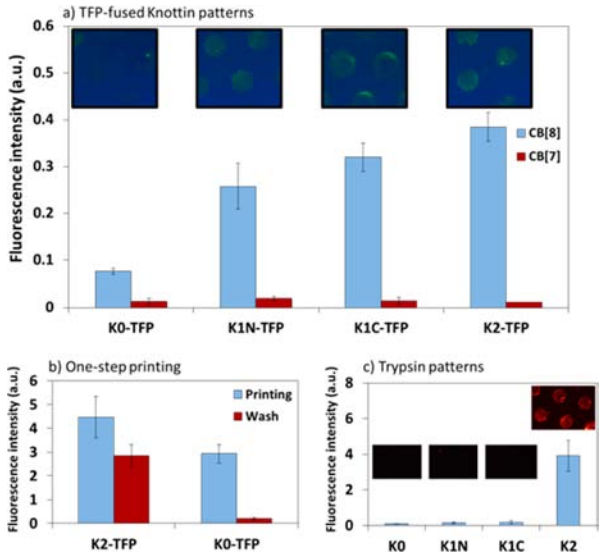

Figure 6. (a) Fluorescence intensity of the different TFP-fused knottins immobilized on surfaces patterned with CB[8] (blue columns) and CB[7] (red columns). (b) Fluorescence intensities of patterns formed by printing a mixture of CB[8] and the TFP-fused knottins (blue columns) and after washing the patterns in buffer for 20 min (red columns). (c) Fluorescence intensities of Tryp-Cy3 immobilized on patterned surfaces of the four different cleaved knottins. Fluorescence intensities of the patterned spots were determined and subtracted from the background in all cases. Data presented as the mean ± STD, $n = 4$.

fluorescent arrays were visible in the cases of both K2-TFP and K0-TFP. After the wash step, 60% of the original fluorescence of the K2-TFP arrays remained, whereas the fluorescence of the K0-TFP arrays almost entirely disappeared (<10% remaining). The final intensity of K2-TFP arrays using this strategy was significantly higher (~7×). Using this strategy, we tested the possibility of binding trypsin to arrays of TFP-cleaved CB[8]-binding knottins. To visualize trypsin on the arrays, we conjugated a Cy3-NHS ester reactive dye to the amino groups of the protein (Tryp-Cy3). Arrays of all four TFP-cleaved knottin constructs were incubated with Tryp-Cy3 for 10 min. Clear Cy3-fluorescent arrays were observed only on surfaces with K2 (Figure 6c). Because of the less stable binding capability of the monovalent CB[8]-binding TFP-cleaved knottins (K1N and K1c), as seen in the SPR measurements, the surface density of K1 constructs is lower after printing and washing, and complete dissociation might have occurred after the complete process. In the case of K2, bivalent interactions result in a higher affinity allowing for a greater surface density of K2 constructs after printing and washing, and slower dissociation during the subsequent steps yields suitable arrays of trypsin binding knottins. These results further highlight that significant differences exist in binding capabilities between monovalent and bivalent guests on ternary-complex forming surfaces. On the basis of these array experiments, we verified the interaction of β-trypsin on a MV^{2+}-CB[8] SAM displaying K2 using SPR (Figure S5). As expected, β-trypsin interacted with this SAM, and rinsing with buffer caused dissociation, confirming that reversible surface adhesion of β-trypsin was achieved through supramolecular interactions.

CONCLUSIONS

CB[8]-binding knottins have been constructed and used to fabricate functional knottin-based supramolecular surfaces that are able to bind their protein binding target. A simple strategy has been developed to recombinantly express and purify knottins by genetically fusing them to TFP using an enterokinase cleavable linker. The TFP-fused knottins have been directly used for fluorescence based analysis and to visualize them on surfaces. Both TFP-fused and TFP-cleaved knottin constructs have been tested for their ability to inhibit β-trypsin and to bind CB[8]. All knottin constructs inhibited β-trypsin with low nanomolar affinities, and those containing CB[8]-binding motifs bound to CB[8] with low micromolar affinities. The knottin constructs have also been immobilized to surfaces displaying MV^{2+} by CB[8]-mediated ternary complex formation. Differences in surface adhesion capabilities were observed between monovalent and bivalent CB[8]-binding knottin constructs. Improved specific binding could be observed when TFP was cleaved off the knottins presumably because of steric hindrance and nonspecific interactions of the TFP with CB[8]. Finally, surface adhesion of trypsin occurred only on surfaces patterned with the divalent knottin construct, K2, due to stronger surface adhesion characteristics.

This study demonstrates, for the first time, the possibility of developing functional knottins that can be incorporated with a supramolecular host−guest system and capture a target protein. Knottins are a robust and versatile class of miniprotein scaffolds for the presentation of high-affinity binding peptides. Knottins that bind biomolecules such as growth factors, hormones, and cell-surface receptors could prove to be powerful components that can be integrated with biologically relevant supramolecular materials like surface coatings, hydrogels, soft nanoparticles, polymers, etc.

EXPERIMENTAL SECTION

Materials. Cucurbit[8]uril, cucurbit[7]uril, β-trypsin from bovine pancreas, and methylviologen were purchased from Sigma-Aldrich. The disulfides (bis-1-(11-{tetraethylene glycol}-undecyl) disulfide and *N*-{2-(2,5-dioxo-2,5-dihydro-pyrrol-1-yl)-ethyl}-[2-[11-(11-(tetraethylene glycol)-undecyldisulfanyl)-undecyloxy]-hexaethylene glycol-acetamide]) for SAM preparation were purchased from ProChimia. Alkyl thiol terminated MV^{2+} (MV-SH) was synthesized as previously reported.[48]

Because of the poor solubility of CB[8] in water and its hygroscopic nature, the apparent molecular weight of the commercial powder and its actual concentration in aqueous solutions were determined for each batch using a simple and highly reproducible method described previously.[49] CB[8] was dissolved in Milli-Q water by sonication at 80 °C for 2 h.

Equipment. Polymerase chain reaction (PCR) was performed using a Peqlab Primus 25 advanced thermocycler. Fast protein liquid chromatography (FPLC) was performed using ÄKTApurifier (GE Healthcare Life Sciences) in combination with a Frac-950 fractionation collector (GE Healthcare Life Sciences). The used column was a Superdex 75 10/300GL (GE Healthcare Life Sciences) and had a separation range for molecules with molecular weights between 3000 and 70000 Da. UV−vis measurements to determine DNA and protein concentrations were performed using a Thermo Scientific Nanodrop 1000. Matrix assisted laser desorption/ionization time-of-flight (MALDI-TOF) analysis was performed with a Waters MALDI SYNAPT high definition mass

DOI: 10.1021/acs.bioconjchem.5b00419
Bioconjugate Chem. 2015, 26, 1972−1980

spectrometer. UV−vis measurements for trypsin inhibitor assays were performed using a PerkinElmer Victor X3 multiwell plate reader. Miscroscale thermophoresis measurements were performed using a Nanotemper Monolith NT.115 device. Surface plasmon resonance (SPR) experiments were conducted using SPR gold substrates (50 nm thickness of gold) from Ssens bv on a Resonant-probes SPR. The reflectivity was measured at fixed angle at which point the linear region of the SPR curve stopped. An Olympus microscope 1 × 71 with appropriate filter settings was used for recording fluorescent images.

Molecular Cloning of Knottin Constructs. A pET15b TFP-Ecoil vector was obtained from W. F. Rurup.[50] ssDNA sequences corresponding to the β-trypsin inhibitor knottin and primers to extend the N- and C-termini with the CB[8]-binding motif, GGWGG, were ordered from Eurofins MWG Operon, Germany. Amplification of the extended genetic construct was performed by PCR using pfu polymerase. The final genetic construct had 5′ BsrGI and 3′ NheI restriction sites, which were used to insert it between the TFP and Ecoil in the plasmid through restriction digestion enzymes and T4 DNA ligase (New England Biolabs inc.). The 3′ terminal also contained a stop codon to prevent expression of the Ecoil leucine zipper. The resulting pET15b TFP-K2 plasmid was transformed into NovaBlue ultracompetent cells (Novagen) and grown overnight on LB agar plates containing 100 mg/L ampicillin. Plasmids were extracted from individual colonies using a Qiagen spin miniprep kit and sequenced by Eurofins MWG Operon, Germany using a standard T7 terminal reverse primer. pET15b TFP-K0, pET15b TFP-K1N, and pET15b TFP-K1C plasmids were constructed by simultaneous site directed mutagenesis (QuickChange Lightning Multi Site-Directed Mutagenesis kit from Agilent Technologies) of the genetic sequences corresponding to both 5′ and 3′ GGWGG motifs to GGGGG. The mutated plasmids were transformed into XL10-Gold ultracompetent cells and grown overnight on LB agar plates containing 34 mg/L chloramphenicol and 100 mg/L ampicillin. Plasmids from several colonies were extracted and sequenced, and bacterial cultures with each of the three different mutation combinations were identified. The four different plasmids were transformed into the expression host, Rosetta-Gami 2(DE3)pLysS competent cells (Novagen), and grown overnight on LB agar plates containing 34 mg/L chloramphenicol and 100 mg/L ampicillin. Individual colonies were grown in LB media containing the mentioned antibiotics. For long-term storage, 15%-glycerol bacterial stocks were made and placed at −80 °C. All genetic sequences, plasmids, and peptide sequences have been provided in the Supporting Information.

Protein Expression and Purification. Five milliliters of bacterial starter cultures was grown overnight from glycerol stocks at 37 °C with shaking in LB media containing appropriate antibiotics. This was then transferred into 1 L of the same media, and the cultures were grown until they attained $O.D._{600\ nm}$ values between 0.4 and 0.8. Protein expression was then induced using isopropyl-β-D-1-thiogalactopyranoside (IPTG) at a final concentration of 0.1 mM. These cultures were grown overnight at 18 °C with shaking. The cultures were then spun down at 6000 rcf for 10 min at 4 °C, and supernatants were discarded. Bacterial pellets were resuspended in 10 mL of BugBuster protein extraction reagent (Novagen) with 10 μL of benzonase (30 U/μL, Novagen) and gently shaken for 20 min at 25 °C. TFP-fused knottin constructs were then purified using His-Select nickel affinity columns (Sigma-Aldrich) into an elution buffer of 50 mM NaH_2PO_2, 300 mM NaCl, and 250 mM imidazole at pH 8. The purified TFP-fused knottins were then rebuffered into pH 7.4 phosphate buffered saline (PBS, Sigma-Aldrich) using 30 kDa-cutoff centrifugal filter units (Amicon Ultra). Concentrations of these TFP-fused knottins were determined from the absorbance value at λ = 467 nm and an extinction coefficient of 64000 M^{-1} cm^{-1}. Knottins were cleaved from the TFP using an enterokinase enzyme (EKMax, Life Technologies). The optimized reaction conditions required 50 ng of protein per 30 μL of reaction with 0.1 units of enterokinase in pH 7.5 buffer containing 20 mM trisHCl, 10 mM NaCl, and 2 mM $CaCl_2$ at 37 °C for 16 h. The cleaved knottin was isolated from the other proteins using a 10 kDa-cutoff centrifugal filter unit (Amicon Ultra) followed by a 3 kDa-cutoff centrifugal filter unit (Amicon Ultra). Final knottin solutions were in PBS. Concentrations of the knottin constructs were determined from the absorbance value at λ = 280 nm and extinction coefficients of 12865 M^{-1} cm^{-1} for K2, 7365 M^{-1} cm^{-1} for K1N and K1C and 1865 M^{-1} cm^{-1} for K0.

Trypsin Inhibitor Assay. Trypsin cleaves peptides and proteins mainly at the carboxyl side of the amino acids lysine or arginine. During this experiment, *N*-benzoyl-L-arginine ethyl ester (BAEE) was used as a substrate for trypsin digestion. This produces an absorbance shift from λ = 230 nm to λ = 253 nm. The rate of reaction was determined for different concentrations of BAEE in the presence and absence of the knottins by following the increase in absorbance using a λ = 260 nm filter. All measurements were performed in PBS.

Microscale Thermophoresis. Solutions containing 1 μM TFP-fused knottins, 150 μM MV, and concentrations of CB[8] ranging from 2 nM to 37.5 μM were made in PBS. Thermophoretic analyses were carried out in standard treated capillaries from Nanotemper using an LED power of 1% and MST power of 80% for 30 s. Thermophoresis was calculated as the ratio of the fluorescence intensity after and before local heating.

Preparation of SAMs on Gold Substrate. Gold substrates were first washed with piranha solution (H_2SO_4 + 30% H_2O_2, v/v 3/1), copious amounts of Milli-Q water, and finally with ethanol. Substrates were then immersed overnight in a 1 mM ethanolic solution of $(EG_4C_{11}S)_2$ and Mal-EG_6C_{11}-S-S-C_{11}-EG_4 at a molar ratio of 99:1 at room temperature in the dark. The substrates were then cleaned thoroughly with ethanol, Milli-Q water, and dried with a stream of N_2 gas. They were then immediately incubated with 1 mM MV-SH in pH 6.8 50 mM phosphate buffer for 1 h. The substrates were then washed thoroughly with Milli-Q water, dried with N_2 gas, and used for further supramolecular assembly experiments.

Surface Plasmon Resonance. Surface adhesion measurements were carried out under conditions of constant flow (100 μL/min) using a pH 7.4 buffer of 0.5 × PBS + 0.05% Tween20. All knottin solutions also contained 50 μM CB[8].

Microcontact Printing. Poly(dimethylsiloxane) (PDMS) stamps were prepared by casting a 10:1 (v/v) mixture of Sylgard 184 elastomer and curing agent (Dow Corning) against a patterned silicon master with 100 μm circles having a depth of 30 μm. After curing the stamps at 60 °C overnight, they were peeled off from the master before using. The individually cut out stamps were O_2-plasma treated for 10 s to form a hydrophilic surface, then inked with the appropriate solution for 20 min after which they were dried with a gentle stream of

DOI: 10.1021/acs.bioconjchem.5b00419
Bioconjugate Chem. 2015, 26, 1972−1980

N_2 gas. These were then stamped on the gold (20 nm thickness) substrate with MV-SAMs for 20 min with a 15 g weight on top. The substrate was then briefly washed with Milli-Q water and dried. In Figure 6a, 100 μM CB[8]/CB[7] in Milli-Q water was printed followed by incubation of the substrate in 1 μM TFP-fused knottin solution for 10 min. The substrates were then briefly washed with Milli-Q water, dried, and imaged. In Figure 6b, a mixture of 50 μM CB[8] with 1 μM TFP-fused knottin was printed for 10 min followed by incubation in buffer containing PBS + 0.1% Tween20 for 20 min with mild shaking. The substrates were then washed with Milli-Q water, dried, and imaged. In Figure 6c, the previous strategy was followed using cleaved knottin solutions, and after the incubation in buffer, the substrates were incubated in a 1 μM Tryp-Cy3 solution for 10 min, then washed with Milli-Q water, dried, and imaged. All proteins including knottin constructs and Tryp-Cy3 were in pH 7.4 buffer containing 0.5 × PBS + 0.05% Tween20.

■ ASSOCIATED CONTENT

Supporting Information

The Supporting Information is available free of charge on the ACS Publications website at DOI: 10.1021/acs.bioconjchem.5b00419.

Genetic and protein sequences, SDS−PAGE, FPLC, MALDI-TOF analyses, UV−vis plot indicating aggregation of cleaved knottins, SPR of TFP-fused knottins, and β-trypsin surface adhesion (PDF)

■ AUTHOR INFORMATION

Corresponding Author

*Tel: +31534892987. E-mail: p.jonkheijm@utwente.nl. Web: www.jonkheijm.org.

Author Contributions

⊥S.S. and M.D.R. contributed equally to this work.

Notes

The authors declare no competing financial interest.

■ ACKNOWLEDGMENTS

We thank Emanuela Cavatorta for providing MV^{2+}-SH, Jenny Brinkmann for providing gold substrates, and Regine van der Hee for her assistance in performing the MALDI-TOF measurements. The facilities of the BioNanoLab of the $MESA^+$ Institute for Nanotechnology are highly appreciated. We also acknowledge funding provided by the European Research Council through Starters grant Sumoman 259183 (to P.J.) and the Dutch Science Foundation through VIDI grant 723.012.106 (to P.J.) of the Council for Chemical Sciences.

■ ABBREVIATIONS

CB[8], Cucurbit[8]uril; K0, β-trypsin inhibitor knottin without the CB[8]-binding motif; K1N, β-trypsin inhibitor knottin with the N-terminal CB[8]-binding motif; K1CN, β-trypsin inhibitor knottin with the C-terminal CB[8]-binding motif; K2, β-trypsin inhibitor knottin with the N-terminal and C-terminal CB[8]-binding motif; TFP, teal fluorescent protein; MV^{2+}, methyl-viologen

■ REFERENCES

(1) Kolmar, H. (2008) Alternative binding proteins: Biological activity and therapeutic potential of cystine-knot miniproteins. *FEBS J. 275*, 2684−2690.

(2) Austin, J., Wang, W., Puttamadappa, S., Shekhtman, A., and Camarero, J. A. (2009) Biosynthesis and biological screening of a genetically encoded library based on the cyclotide MCoTI-I. *ChemBioChem 10*, 2663−2670.

(3) Gelly, J., Gracy, J., Kaas, Q., Le-Nguyen, D., Heitz, A., and Chiche, L. (2004) The KNOTTIN website and database: a new information system dedicated to the knottin scaffold. *Nucleic Acids Res. 32*, 156D−159D.

(4) Gracy, J., Le-Nguyen, D., Gelly, J.-C., Kaas, Q., Heitz, A., and Chiche, L. (2008) KNOTTIN: the knottin or inhibitor cystine knot scaffold in 2007. *Nucleic Acids Res. 36*, D314−D319.

(5) Gould, A., Ji, Y., Aboye, T. L., and Camarero, J. A. (2011) Cyclotides, a novel ultrastable polypeptide scaffold for drug discovery. *Curr. Pharm. Des. 17*, 4294−4307.

(6) Moore, S. J., Leung, C. L., and Cochran, J. R. (2012) Knottins: disulfide-bonded therapeutic and diagnostic peptides. *Drug Discovery Today: Technol. 9*, e3−e11.

(7) Banta, S., Dooley, K., and Shur, O. (2013) Replacing antibodies: engineering new binding proteins. *Annu. Rev. Biomed. Eng. 15*, 93−113.

(8) Hosse, R. J., Rothe, A., and Power, B. E. (2006) A new generation of protein display scaffolds for molecular recognition. *Protein Sci. 15*, 14−27.

(9) Getz, J. A., Rice, J. J., and Daugherty, P. S. (2011) Protease-resistant peptide ligands from a knottin scaffold library. *ACS Chem. Biol. 6*, 837−844.

(10) Getz, J. A., Cheneval, O., Craik, D. J., and Daugherty, P. S. (2013) Design of a cyclotide antagonist of neuropilin-1 and −2 that potently inhibits endothelial cell migration. *ACS Chem. Biol. 8*, 1147−1154.

(11) Heitz, A., Le-Nguyen, D., and Chiche, L. (1999) Min-21 and Min-23, the smallest peptides that fold like a cystine-stabilized β-sheet motif: design, solution structure, and thermal stability. *Biochemistry 38*, 10615−10625.

(12) Souriau, C., Chiche, L., Irving, R., and Hudson, P. (2005) New binding specificities derived from Min-23, a small cystine-stabilized peptidic scaffold. *Biochemistry 44*, 7143−7155.

(13) Chang, H.-J., Hsu, H.-J., Chang, C.-F., Peng, H.-P., Sun, Y.-K., Yu, H.-M., Shih, H.-C., Song, C.-Y., Lin, Y.-T., Chen, C.-C., et al. (2009) Molecular evolution of cystine-stabilized miniproteins as stable proteinaceous binders. *Structure 17*, 620−631.

(14) Huang, Y.-J., Chen, I.-C., Yu, C.-M., Lee, Y.-C., Hsu, H.-J., Ching, A. T. C., Chang, H.-J., and Yang, A.-S. (2010) Engineering anti-vascular endothelial growth factor single chain disulfide-stabilized antibody variable fragments (sc-dsFv) with phage-displayed sc-dsFv libraries. *J. Biol. Chem. 285*, 7880−7891.

(15) Silverman, A. P., Levin, A. M., Lahti, J. L., and Cochran, J. R. (2009) Engineered cystine-knot peptides that Bind $\alpha v\beta 3$ integrin with antibody-like affinities. *J. Mol. Biol. 385*, 1064−1075.

(16) Kimura, R. H., Levin, A. M., Cochran, F. V., and Cochran, J. R. (2009) Engineered cystine knot peptides that bind $\alpha v\beta 3$, $\alpha v\beta 5$, and $\alpha 5\beta 1$ integrins with low-nanomolar affinity. *Proteins: Struct., Funct., Genet. 77*, 359−369.

(17) Kim, J. W., Cochran, F. V., and Cochran, J. R. (2015) A chemically cross-linked knottin dimer binds integrins with picomolar affinity and inhibits tumor cell migration and proliferation. *J. Am. Chem. Soc. 137*, 6−9.

(18) Jagadish, K., Borra, R., Lacey, V., Majumder, S., Shekhtman, A., Wang, L., and Camarero, J. A. (2013) Expression of fluorescent cyclotides using protein trans-splicing for easy monitoring of cyclotide−protein interactions. *Angew. Chem., Int. Ed. 52*, 3126−3131.

(19) Kimura, R. H., Cheng, Z., Gambhir, S. S., and Cochran, J. R. (2009) Engineered knottin peptides: a new class o f agents for imaging integrin expression in living subjects. *Cancer Res. 69*, 2435−2442.

(20) Miao, Z., Ren, G., Liu, H., Kimura, R. H., Jiang, L., Cochran, J. R., Gambhir, S. S., and Cheng, Z. (2009) An engineered knottin peptide labeled with 18F for PET imaging of integrin expression. *Bioconjugate Chem. 20*, 2342−2347.

(21) Cabanas-Danés, J., Rodrigues, E. D., Landman, E., van Weerd, J., van Blitterswijk, C., Verrips, T., Huskens, J., Karperien, M., and

DOI: 10.1021/acs.bioconjchem.5b00419
Bioconjugate Chem. 2015, 26, 1972−1980

Jonkheijm, P. (2014) A supramolecular host−guest carrier system for growth factors employing VHH fragments. *J. Am. Chem. Soc. 136*, 12675−12681.
(22) Kehr, N. S., Atay, S., and Ergün, B. (2015) Self-assembled monolayers and nanocomposite hydrogels of functional nanomaterials for tissue engineering applications. *Macromol. Biosci. 15*, 445−463.
(23) Wu, G., Li, P., Feng, H., Zhang, X., and Chu, P. K. (2015) Engineering and functionalization of biomaterials via surface modification. *J. Mater. Chem. B 3*, 2024−2042.
(24) Elemans, J. A. A. W., Lei, S., and De Feyter, S. (2009) Molecular and supramolecular networks on surfaces: from two-dimensional crystal engineering to reactivity. *Angew. Chem., Int. Ed. 48*, 7298−7332.
(25) Uhlenheuer, D. A., Petkau, K., and Brunsveld, L. (2010) Combining supramolecular chemistry with biology. *Chem. Soc. Rev. 39*, 2817−2826.
(26) Brinkmann, J., Cavatorta, E., Sankaran, S., Schmidt, B., van Weerd, J., and Jonkheijm, P. (2014) About supramolecular systems for dynamically probing cells. *Chem. Soc. Rev. 43*, 4449−4469.
(27) Ma, X., and Zhao, Y. (2014) Biomedical applications of supramolecular systems based on host−guest interactions. *Chem. Rev. 115*, 7794.
(28) Boekhoven, J., and Stupp, S. I. (2014) Supramolecular materials for regenerative medicine. *Adv. Mater. 26*, 1642−1659.
(29) An, Q., Brinkmann, J., Huskens, J., Krabbenborg, S., de Boer, J., and Jonkheijm, P. (2012) A supramolecular system for the electrochemically controlled release of cells. *Angew. Chem., Int. Ed. 51*, 12233−12237.
(30) Boekhoven, J., Rubert Pérez, C. M., Sur, S., Worthy, A., and Stupp, S. I. (2013) Dynamic display of bioactivity through host−guest chemistry. *Angew. Chem., Int. Ed. 52*, 12077−12080.
(31) Voskuhl, J., Sankaran, S., and Jonkheijm, P. (2014) Optical control over bioactive ligands at supramolecular surfaces. *Chem. Commun. 50*, 15144−15147.
(32) Sankaran, S., Kiren, M. C., and Jonkheijm, P. (2015) Incorporating bacteria as a living component in supramolecular self-assembled monolayers through dynamic nanoscale interactions. *ACS Nano 9*, 3579−3586.
(33) Masson, E., Ling, X., Joseph, R., Kyeremeh-Mensah, L., and Lu, X. (2012) Cucurbituril chemistry: a tale of supramolecular success. *RSC Adv. 2*, 1213−1247.
(34) Lee, J. W., Samal, S., Selvapalam, N., Kim, H.-J., and Kim, K. (2003) Cucurbituril homologues and derivatives: new opportunities in supramolecular chemistry. *Acc. Chem. Res. 36*, 621−630.
(35) Liu, S., Zavalij, P. Y., and Isaacs, L. (2005) Cucurbit[10]uril. *J. Am. Chem. Soc. 127*, 16798−16799.
(36) Lagona, J., Mukhopadhyay, P., Chakrabarti, S., and Isaacs, L. (2005) The cucurbit[n]uril family. *Angew. Chem., Int. Ed. 44*, 4844−4870.
(37) Stoffelen, C., Voskuhl, J., Jonkheijm, P., and Huskens, J. (2014) Dual stimuli-responsive self-assembled supramolecular nanoparticles. *Angew. Chem., Int. Ed. 53*, 3400−3404.
(38) Hu, C., Lan, Y., Tian, F., West, K. R., and Scherman, O. A. (2014) Facile method for preparing surface-mounted cucurbit[8]uril-based rotaxanes. *Langmuir 30*, 10926−10932.
(39) González-Campo, A., Brasch, M., Uhlenheuer, D. A., Gómez-Casado, A., Yang, L., Brunsveld, L., Huskens, J., and Jonkheijm, P. (2012) Supramolecularly oriented immobilization of proteins using cucurbit[8]uril. *Langmuir 28*, 16364−16371.
(40) Brinkmann, J., Sankaran, S., Rinnen, S., Arlinghaus, F. H., De Boer, J., and Jonkheijm, P. (2015) Cellular responses to dynamic reversible interfaces employing supramolecular cucurbit[8]uril-mediated RGD ligand assembly, unpublished work.
(41) Bush, M. E., Bouley, N. D., and Urbach, A. R. (2005) Charge-mediated recognition of N-terminal tryptophan in aqueous solution by a synthetic host. *J. Am. Chem. Soc. 127*, 14511−14517.
(42) Schmoldt, H.-U., Wentzel, A., Becker, S., and Kolmar, H. (2005) A fusion protein system for the recombinant production of short disulfide bond rich cystine knot peptides using barnase as a purification handle. *Protein Expression Purif. 39*, 82−89.
(43) Bode, W., Greyling, H. J., Huber, R., Otlewski, J., and Wilusz, T. (1989) The refined 2.0 A X-ray crystal structure of the complex formed between bovine beta-trypsin and CMTI-I, a trypsin inhibitor from squash seeds (Cucurbita maxima). Topological similarity of the squash seed inhibitors with the carboxypeptidase A inhibitor from potatoes. *FEBS Lett. 242*, 285−292.
(44) Morrison, J. F. (1969) Kinetics of the reversible inhibition of enzyme-catalysed reactions by tight-binding inhibitors. *Biochim. Biophys. Acta BBA - Enzymol 185*, 269−286.
(45) Uhlenheuer, D. A., Wasserberg, D., Haase, C., Nguyen, H. D., Schenkel, J. H., Huskens, J., Ravoo, B. J., Jonkheijm, P., and Brunsveld, L. (2012) Directed supramolecular surface assembly of SNAP-tag fusion proteins. *Chem. - Eur. J. 18*, 6788−6794.
(46) Nguyen, H. D., Dang, D. T., van Dongen, J. L. J., and Brunsveld, L. (2010) Protein dimerization induced by supramolecular interactions with cucurbit[8]uril. *Angew. Chem. 122*, 907−910.
(47) Voskuhl, J., Brinkmann, J., and Jonkheijm, P. (2014) Advances in contact printing technologies of carbohydrate, peptide and protein arrays. *Curr. Opin. Chem. Biol. 18*, 1−7.
(48) Tian, F., Cheng, N., Nouvel, N., Geng, J., and Scherman, O. A. (2010) Site-Selective Immobilization of colloids on Au substrates via a noncovalent supramolecular "Handcuff". *Langmuir 26*, 5323−5328.
(49) Yi, S., and Kaifer, A. E. (2011) Determination of the purity of cucurbit[n]uril (n = 7, 8) host samples. *J. Org. Chem. 76*, 10275−10278.
(50) Rurup, W. F., Verbij, F., Koay, M. S. T., Blum, C., Subramaniam, V., and Cornelissen, J. J. L. M. (2014) Predicting the loading of virus-like particles with fluorescent proteins. *Biomacromolecules 15*, 558−563.

DOI: 10.1021/acs.bioconjchem.5b00419
Bioconjugate Chem. 2015, 26, 1972−1980